




A NEW IMPROVED CONTROL FOR POWER QUALITY ENHANCEMENT IN DOUBLE FED INDUCTION GENERATOR USING ITERATIVE LEARNING CONTROL

Oussama DJAIDJA ^{1,*}, Hemza MEKKI ², Samir ZEGHLACHE ¹, Ali DJERIOUI ² 

¹ Laboratoire d'Analyse des Signaux et Systèmes, Department of Electrical Engineering, University of M'Sila, Algeria

² Laboratoire de Génie Electrique, Department of Electrical Engineering, Faculty of Technology, University Mohamed Boudiaf of M'Sila, Algeria

*Corresponding author, e-mail: oussama.djaidja@univ-msila.dz

Abstract

This work presents a new Fault Tolerant Control approach for a doubly fed induction generator using Iterative Learning Control when the fault occurs. The goal of this research is to apply the proposed ILC controller in conjunction with vector control for doubly fed induction generator to enhance its reliability and availability under broken rotor bars. However, the performances of classical VC control are often characterized by their inability to deal with the effects of faults. To overcome these drawbacks, a combination of VC control and iterative learning control is described. The input control signal of the VC controller is gradually regulated by the ILC harmonic compensator in order to eliminate the faults effect. The improvement of this approach related to active and reactive power ripples overshoot and response time have been explained. Which active and reactive power response time have been reduced more than 84% and 87.5 % respectively. The active and reactive power overshoots have been reduced about 45% and 35% respectively. The obtained results emphasize the efficiency and the ability of the proposed FTC to enhance the power quality in faulty condition.

Keywords: doubly fed induction generator, vector control, fault tolerant control, iterative learning control, broken rotor bars

List of Symbols/Acronyms

AFTC – Active Fault Tolerant Control
BRB – Broken Rotor Bars
DFIG – Doubly Fed Induction Generator
FDI – Fault Detection and Isolation
FTC – Fault Tolerant Control
ILC – Iterative Learning Control
PFTC – Passive Fault Tolerant Control
SVM – Space Vector Modulation
VC – Vector Control

1. INTRODUCTION

In the last few decade, The Doubly-fed Induction Generator has gained more interest in large wind turbine because of their reliability, robustness, reduced inverter costs, power control capability and full variable speed operation [1]. Despite these advantages, this kind of generator can be affected by several faults that deteriorate their performances, which are current sensor faults, short circuit and rotor failures including broken rotor bars [2]-[3], the broken rotor bars is one of the most common faults in DFIG, it can be created by mechanical cracks or overloads. To overcome this drawback we use the fault tolerant control [4].

The fault tolerant control is the best choice for eliminating previous fault because it allows a system to keep operating even the occurrence of faults, therefore the application of FTC on DFIG provides significant economic benefits to the wind turbine [5]. Much researchers classifies fault tolerant control into two parts [6], the first called active fault tolerant control (AFTC) and the second called passive fault tolerant control (PFTC). The AFTC aims to ensure the stability and performance, by modifying online the parameters or the structure of the controller. This solution requires to be reconfigured based on the block information given for fault detection and isolation on (FDI) [7]-[8], in other hand the passive approach uses a robust controller that can maintain good performance when faults occur; unlike the active approach, this method does not require fault detection and isolation blocks. The PFTC can avoid the time required in the AFTC for online diagnostics and design monitoring, which is very necessary in practical situations [9]-[10].

In recent years, the power quality is still a big challenge. Hence, many research publications have studied the improvement of the power quality using VC controller. This approach are frequently utilized

Received 2023-03-07; Accepted 2023-07-10; Available online 2023-08-21

© 2023 by the Authors. Licensee Polish Society of Technical Diagnostics (Warsaw, Poland). This article is an open access article distributed under the terms and conditions of the Creative Commons Attribution (CC BY) license (<http://creativecommons.org/licenses/by/4.0/>).

in wind turbines because they have the ability to adjust the DFIG model [11]-[12]. In [13], authors present an improvement of the power derived from wind energy, using direct and indirect vector control, taking into account the variation of wind speed that causes a challenge in energy production. In addition, the work in [14] proposes a new direct vector control (DVC) for a doubly fed induction generator (DFIG) based on space vector modulation (SVM) using in a wind turbine system (WTS). However, the VC control method has poor performance and low robustness when faults occur. Thus, in our paper an effective Fault Tolerant Control (FTC) approach for power quality enhancement in a doubly-fed induction generator is designed. The proposed technique is based on combining an iterative learning controller (ILC) with VC control under the rotor faults. This approach is favourable for industrial power implementations due to its effectiveness and robustness in critical process situations. The ILC technique has broad interest by researchers in systems subjected to periodic faults, because this strategy can modify the input signal repeatedly when the monitoring task is performed in order to get high disturbance rejection [15]-[16]. In [15] two iterative learning control techniques applied in the time and frequency domains, respectively, have been presented to minimize periodic speed ripples caused by torque pulsations. The authors in [16] develop an effective control approach for improving power quality in a four-leg inverter-based standalone system. The suggested scheme combines a sliding mode controller (SMC) with an iterative learning controller (ILC) for harmonic compensation.

In this work, a new combined VC-ILC approach for doubly-fed induction generator has been presented and investigated. The DFIG model and more details of the suggested control technique have been explicated. Active and reactive power ripples, overshoot and time response improvement, and accuracy have all been demonstrated and compared.

The remainder of this article is structured as follows: first the mathematical model of the doubly-fed induction generator (DFIG) and the Vector control for active and reactive power controllers is presented in Section 2. Section 3 discusses, the defective model of DFIG. Section 4 develops the proposed FTC (VC-ILC). The simulation results are reported in Section 5. Section 6 gives some concluding remarks.

2. MATHEMATICAL MODELS

The mathematical model of a Doubly Fed Induction Generator (DFIG) comprises equations for the stator and rotor windings, the magnetic flux, and the electromagnetic torque. The mathematical model is critical for understanding the behavior of DFIGs and for enhancing their performance in wind power systems.

2.1. DFIG Model

The DFIG's voltage and flux equations in the park reference are illustrated in Eq. as follows [17]

$$V_{dr} = R_r I_{dr} + \frac{d}{dt} \varphi_{dr} - w_r \varphi_{qr} \quad (1)$$

$$V_{qr} = R_r I_{qr} + \frac{d}{dt} \varphi_{qr} + w_r \varphi_{dr} \quad (2)$$

$$V_{ds} = R_s I_{ds} + \frac{d}{dt} \varphi_{ds} - w_s \varphi_{qs} \quad (3)$$

$$V_{qs} = R_s I_{qs} + \frac{d}{dt} \varphi_{qs} + w_s \varphi_{ds} \quad (4)$$

And

$$\varphi_{dr} = L_r I_{dr} + M I_{ds} \quad (5)$$

$$\varphi_{qr} = L_r I_{qr} + M I_{qs} \quad (6)$$

$$\varphi_{ds} = L_s I_{ds} + M I_{dr} \quad (7)$$

$$\varphi_{qs} = L_s I_{qs} + M I_{qr} \quad (8)$$

The equation below gives the electromagnetic torque

$$T_e = p \frac{M}{L_s} (I_{dr} \varphi_{qs} - I_{qr} \varphi_{ds}) \quad (9)$$

Where : L_s , L_r and M are stator, rotor and mutual inductances, I_{dr} and I_{qr} are rotor current components, I_{ds} and I_{qs} are stator current components, R_s and R_r are the stator and rotor resistance, V_{ds} and V_{qs} are stator voltage components, V_{dr} and V_{qr} are rotor voltage components, indexes d, q stand for the direct and quadrature components. w_s and w_r are the synchronous and rotor speed, T_e is the electromagnetic torque, φ_{ds} , φ_{qs} , φ_{qr} and φ_{dr} are the stator and the rotor fluxes, σ is the coefficient of dispersion f is the viscous friction coefficient, J is the inertia, and p is the number of pole pairs.

The equations below represent the classical modelling of the doubly fed induction generator [18].

$$\begin{aligned} \frac{d}{dt} I_{dr} = & \frac{M \cdot R_s}{L_r L_s \sigma} \cdot I_{ds} - \frac{M}{L_r \sigma} \cdot w_s \cdot I_{qs} + \frac{M}{L_r \sigma} \cdot w_r \cdot I_{qs} \\ & - \frac{1}{\sigma L_r} R_r I_{dr} + \\ & + \frac{1}{\sigma} \cdot w_r \cdot I_{qr} - \frac{M^2}{L_r L_s \sigma} \cdot w_s \cdot I_{qr} - \frac{M}{L_r L_s \sigma} V_{ds} + \frac{1}{\sigma L_r} V_{dr} \end{aligned} \quad (10)$$

$$\begin{aligned} \frac{d}{dt} I_{qr} = & \frac{M}{L_r \sigma} \cdot w_s \cdot I_{ds} - \frac{M}{L_r \sigma} \cdot w_r \cdot I_{ds} + \frac{M \cdot R_s}{L_r L_s \sigma} \cdot I_{qs} \\ & + \frac{M^2}{L_r L_s \sigma} \cdot w_s \cdot I_{dr} + \\ & - \frac{1}{\sigma} \cdot w_r \cdot I_{dr} - \frac{1}{\sigma L_r} \cdot R_r \cdot I_{qr} - \frac{M}{L_r L_s \sigma} \cdot V_{qs} + \frac{1}{\sigma L_r} \cdot V_{qr} \end{aligned} \quad (11)$$

$$\begin{aligned} \frac{d}{dt} I_{ds} = & - \frac{R_s}{\sigma \cdot L_s} \cdot I_{ds} + \frac{1}{\sigma} \cdot w_s \cdot I_{qs} - \frac{M^2 w_r}{L_r L_s \sigma} \cdot I_{qs} \\ & + \frac{M}{L_r L_s \sigma} \cdot R_r \cdot I_{dr} + \\ & - \frac{M}{L_s \sigma} \cdot w_r \cdot I_{qr} + \frac{M}{L_s \sigma} \cdot w_s \cdot I_{qr} + \frac{1}{\sigma L_s} \cdot V_{ds} - \frac{M}{L_r L_s \sigma} \cdot V_{dr} \end{aligned} \quad (12)$$

$$\begin{aligned} \frac{d}{dt} I_{qs} = & - \frac{R_s}{\sigma \cdot L_s} \cdot I_{qs} + \frac{1}{\sigma} \cdot w_s \cdot I_{ds} + \frac{M^2 w_r}{L_r L_s \sigma} \cdot w_r \cdot I_{ds} \\ & + \frac{M}{L_s \sigma} \cdot w_r \cdot I_{dr} + \\ & + \frac{M}{L_r L_s \sigma} \cdot R_r \cdot I_{qr} - \frac{M}{L_s \sigma} \cdot w_s \cdot I_{dr} + \frac{1}{\sigma L_s} \cdot V_{qs} - \frac{M}{L_r L_s \sigma} \cdot V_{qr} \end{aligned} \quad (13)$$

Where:

$$\sigma = \frac{1-M^2}{L_s L_r}$$

The equations of the Active and reactive stator powers are:

$$\begin{cases} P_s = \frac{3}{2}(V_{ds}I_{ds} + V_{qs}I_{qs}) \\ Q_s = \frac{3}{2}(V_{qs}I_{ds} - V_{ds}I_{qs}) \end{cases} \quad (14)$$

2.2. Vector Control

Vector control is among the best choice utilised for electrical devices. It is predicated on the idea that the system is identical to a separate excitation DC machine [13]. In this situation, we suggested a DFIG control rule based on the orientation of the stator flux, which is employed to operate a generator. The latter emphasizes the relation between the stator and rotor components. These connections can help in acting on rotor signals to regulate the interchange of active and reactive power between the machine's stator and the grid. It can be described in the following state equations whose: $\varphi_{ds} = \varphi_s$ and $\varphi_{qs} = 0$, with neglecting the winding stator resistance R_s [14].

$$\begin{cases} V_{ds} = 0 \\ V_{qs} = V_s = w_s \varphi_s \\ V_{dr} = R_r \cdot I_{dr} + \frac{d\varphi_{dr}}{dt} - w_r \varphi_{qr} \\ V_{qr} = R_r \cdot I_{qr} + \frac{d\varphi_{qr}}{dt} - w_r \varphi_{dr} \end{cases} \quad (15)$$

In addition, the flux is expressed by:

$$\begin{cases} \varphi_{ds} = \varphi_s = L_s \cdot I_{ds} + M \cdot I_{dr} \\ 0 = L_s \cdot I_{qs} + M \cdot \varphi_{qr} \\ \varphi_{dr} = L_r \cdot I_{dr} + M \cdot \varphi_{ds} \\ \varphi_{qr} = L_r \cdot I_{qr} + M \cdot \varphi_{qs} \end{cases} \quad (16)$$

The equations below represent the stator powers and rotor currents:

$$\begin{cases} P_s = -\frac{V_s M}{L_s} \cdot I_{qr} \\ Q_s = \frac{V_s^2}{w_s L_s} - \frac{V_s M}{L_s} \cdot I_{dr} \end{cases} \quad (17)$$

$$\begin{cases} I_{qr} = -\frac{L_s}{V_s M} \cdot P_s \\ I_{dr} = \frac{V_s^2}{w_s L_s} - \frac{L_s}{V_s M} \cdot Q_s \end{cases} \quad (18)$$

The control voltages obtained are expressed by the equations as follows:

$$\begin{cases} V_{dr} = \left[R_r + \left(L_r - \frac{M^2}{L_s} \right) s \right] I_{dr} - g w_s \left(L_r - \frac{M^2}{L_s} \right) \cdot I_{qr} \\ V_{qr} = \left[R_r + \left(L_r - \frac{M^2}{L_s} \right) s \right] I_{qr} + g w_s \left(L_r - \frac{M^2}{L_s} \right) I_{dr} + g \frac{V_s M}{L_s} \end{cases} \quad (19)$$

In figure 1. It presents the block diagram of vector control applied to doubly fed induction generator.

3. DFIG FAULTY MODEL

This part represents the model of DFIG in the event of rotor faults. According to [5], the occurrence of these faults generates asymmetry in the DFIG and makes harmonics in the stator windings, so a sinusoidal component of pulsation $\omega_i = 2\pi f_i$ is added to the quadratic and direct components of stator current. The following ecosystem represents the sinusoidal components that caused by the occurrence of faults [19]-[20]

$$\dot{w} = S(\omega) \cdot w \quad w \in \mathfrak{R}^{4n_f+2} \quad (20)$$

With

$$\omega = (\omega_1 \quad \omega_{-1} \quad \dots \quad \omega_{n_f} \quad \omega_{-n_f})$$

Where

ω : The pulsations vector, n_f : The broken bars faults numbers

$$\begin{aligned} S(\omega) &= \text{diag}(S_{r,1}, \dots, S_{r,n_f}) \\ S_{r,k} &= \text{diag} \left(\begin{pmatrix} 0 & \omega_k \\ -\omega_k & 0 \end{pmatrix}, \begin{pmatrix} 0 & \omega_{-k} \\ -\omega_{-k} & 0 \end{pmatrix} \right) \end{aligned} \quad (21)$$

Where $\omega_{\pm k}$, $k = 1, \dots, n_f$ are the pulsations of the harmonics caused by the rotor faults. Faults created by broken bars produce harmonics component at the frequency as explained in:

$$f_{r,k} = (1 \pm 2ks_w)f \quad (22)$$

Where s_w : The slip ($s_w = \omega_s - \omega$), f : The supply frequency, k : Positive integer ($k = 1, \dots, n_f$)

The harmonics' amplitudes and phases are unknown; they depend on the initial state $w(0)$ of the ecosystem. Then, the additive sinusoidal terms can be as a suitable combination of the ecosystem state, i.e:

$$\begin{cases} i_{sd} \rightarrow i_{sd} + Q_d w \\ i_{sq} \rightarrow i_{sq} + Q_q w \end{cases} \quad (23)$$

With

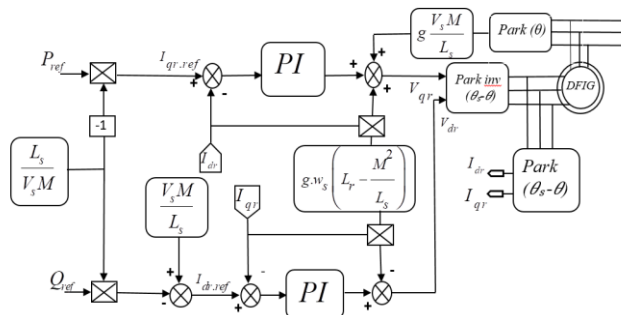


Fig. 1. Block diagram of VC applied to DFIG [17]

$$\begin{cases} Q_d = (1 & 0 & 1 & 0 & \dots & 1 & 0) \\ Q_q = (0 & 1 & 0 & 1 & \dots & 0 & 1) \end{cases}$$

The derivative of (23) is given by

$$\begin{cases} \frac{dI_{ds}}{dt} \rightarrow \frac{dI_{ds}}{dt} + Q_d \cdot S \cdot w \\ \frac{dI_{qs}}{dt} \rightarrow \frac{dI_{qs}}{dt} + Q_q \cdot S \cdot w \end{cases} \quad (24)$$

After introducing the additive perturbing terms $Q_d w$ and $Q_q w$ and their derivatives $Q_d \cdot S \cdot w, Q_q \cdot S \cdot w$, respectively, we get the new state equations defining the DFIG faulty model:

$$\begin{aligned} \frac{d}{dt} I_{dr} = & \frac{M \cdot R_s}{L_r L_s \sigma} \cdot I_{ds} - \frac{M}{L_r \sigma} \cdot \omega_s \cdot I_{qs} + \frac{M}{L_r \sigma} \cdot \omega_r \cdot I_{qs} \\ & - \frac{1}{\sigma L_r} R_r I_{dr} + \\ & + \frac{1}{\sigma} \cdot \omega_r \cdot I_{qr} - \frac{M^2}{L_r L_s \sigma} \cdot \omega_s \cdot I_{qr} - \frac{M}{L_r L_s \sigma} V_{ds} + \frac{1}{\sigma L_r} V_{dr} + \\ & \Gamma_{dr} \cdot w \end{aligned} \quad (25)$$

$$\begin{aligned} \frac{d}{dt} I_{qr} = & \frac{M}{L_r \sigma} \cdot \omega_s \cdot I_{ds} - \frac{M}{L_r \sigma} \cdot \omega_r \cdot I_{ds} + \frac{M \cdot R_s}{L_r L_s \sigma} \cdot I_{qs} \\ & + \frac{M^2}{L_r L_s \sigma} \cdot \omega_s \cdot I_{dr} + \\ & - \frac{1}{\sigma} \cdot \omega_r \cdot I_{dr} - \frac{1}{\sigma L_r} \cdot R_r \cdot I_{qr} - \frac{M}{L_r L_s \sigma} \cdot V_{qs} + \frac{1}{\sigma L_r} \cdot V_{qr} + \\ & \Gamma_{qr} \cdot w \end{aligned} \quad (26)$$

$$\begin{aligned} \frac{d}{dt} I_{ds} = & -\frac{R_s}{\sigma \cdot L_s} \cdot I_{ds} + \frac{1}{\sigma} \cdot \omega_s \cdot I_{qs} - \frac{M^2 w_r}{L_r L_s \sigma} \cdot I_{qs} \\ & + \frac{M}{L_r L_s \sigma} \cdot R_r \cdot I_{dr} + \\ & - \frac{M}{L_s \sigma} \cdot \omega_r \cdot I_{qr} + \frac{M}{L_s \sigma} \cdot \omega_s \cdot I_{qr} + \frac{1}{\sigma L_s} \cdot V_{ds} - \frac{M}{L_r L_s \sigma} \cdot V_{dr} + \\ & \Gamma_{ds} \cdot w \end{aligned} \quad (27)$$

$$\begin{aligned} \frac{d}{dt} I_{qs} = & -\frac{R_s}{\sigma \cdot L_s} \cdot I_{qs} + \frac{1}{\sigma} \cdot \omega_s \cdot I_{ds} + \frac{M^2 w_r}{L_r L_s \sigma} \cdot \omega_r \cdot I_{ds} \\ & + \frac{M}{L_s \sigma} \cdot \omega_r \cdot I_{dr} + \\ & + \frac{M}{L_r L_s \sigma} \cdot R_r \cdot I_{qr} - \frac{M}{L_s \sigma} \cdot \omega_s \cdot I_{dr} + \frac{1}{\sigma L_s} \cdot V_{qs} - \frac{M}{L_r L_s \sigma} \cdot V_{qr} + \\ & \Gamma_{qs} \cdot w \end{aligned} \quad (28)$$

Where: $\Gamma_{ds}, \Gamma_{qs}, \Gamma_{dr}$, and Γ_{qr} describe the fault terms, presented by:

$$\begin{cases} \Gamma_{dr} = a_5 Q_d + a_6 \omega_s Q_q + a_6 \omega_r Q_q \\ \Gamma_{qr} = a_6 \omega_s Q_d - a_6 \omega_r Q_d + a_5 Q_q \\ \Gamma_{ds} = -a_0 Q_d + b_1 \omega_s Q_q - a_1 Q_q - Q_d S \\ \Gamma_{qs} = -a_0 Q_q + b_1 \omega_s Q_d - a_1 \omega_r Q_q - Q_q S \end{cases} \quad (29)$$

4. FAULT-TOLERANT CONTROL STRATEGY

4.1. ILC Approach For DFIG

Iterative learning control is a method for enhancing the monitoring efficiency of machines, which function in a repetitive manner over a set length of time. It is beneficial for problems where a system needs to handle various kinds of inputs in the face of modeling uncertainty, design uncertainty, or system nonlinearities in response to periodic input disturbances. The iterative learning controller

calculates the error that is saved in the memory for use in the following cycle of operation. [15]- [21]- [22]. The proposed ILC approach is shown in Figure 2, with the learning law as follows:

$$v_{i+1}(t) = (1 - \alpha)v_i(t) + \Phi \varepsilon_i(t) + \Gamma \varepsilon_{i+1}(t) \quad (30)$$

Where $v_i(t)$ is the control signal that generated from ILC, α is the forgetting factor, $\varepsilon_i(t)$ is the error signal of the active power with $p_s^*(t) - p_s(t)$, $i = 1, 2, 3, \dots$ is the iteration number, Γ and Φ are the previous and current cycle feedback gains, respectively. (See [15]-[16] for more information about determining the learning gains Φ and Γ). Figure. 3 describes the overall block diagram of the combination between VC and the proposed control strategy (VC-ILC). When the system is subjected to critical disturbances that can deteriorate the overall system performances. Therefore, the suggested approach can change the input control trajectories when the control operation is repeated, with the objective of converging to zero tracking error, in the meantime, the proposed ILC controller exploits undesirable output voltage disturbances, whose frequencies are encompassed within the bandwidth of the vector controller.

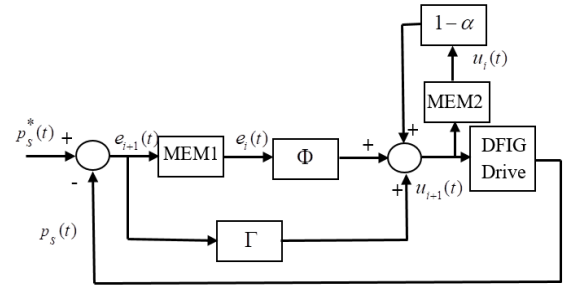


Fig. 2. Block diagram of the ILC scheme [15]

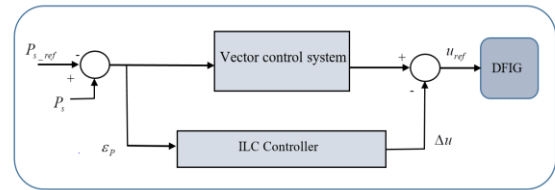


Fig. 3. Block diagram of the classical control (VC) combined with the proposed strategy (ILC)

5. SIMULATION RESULT AND INTERPRETATION

In order to validate the feasibility and robustness of the suggested approach in faulty operation as illustrated in the preceding section, we show some tests of the MATLAB/Simulink for a doubly fed induction generator, that is under the load torque equal 10 Nm applied at $t = 2s$ whose nominal electrical and mechanical parameters are given in Table 1.

Table 1. DFIG parameters

Parameters	Definition	Value	Unit
P_n	Nominal power	3	KW
F	Stator frequency	50	Hz
V	Stator voltage	220	V
L_s	Stator inductance	0.084	H
L_r	Rotor inductance	0.081	H
L_m	Mutual inductance	0.078	H
R_s	Stator resistance	0.455	Ω
R_r	Rotor resistance	0.6	Ω
J	Inertia	0.3125	$Kg.m^2$
f_v	Viscous friction	0.00673	$Kg.m^2/s$
P	Number of pole pairs.	2	

The Vector control and the suggested VC-ILC are used to assess the performance of the DFIG when the faults occur. Figure 4. reveals the efficiency of the proposed VC-ILC compared to the traditional power trajectories converge to their desired VC when the DFIG is subjected to rotor faults.

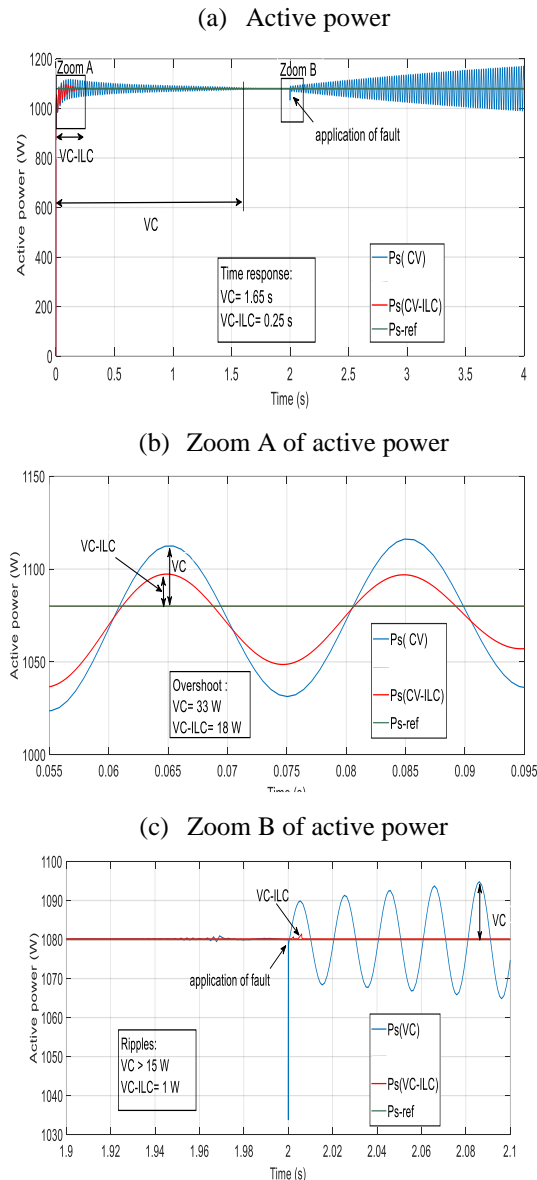


Fig. 4. Active power signals with VC and proposed VC-ILC controller in faulty condition

We can observe that the Active and the reactive references with satisfactory dynamics, when the proposed VC-ILC is applied unlike the traditional VC that appears high ripples.

Depending on Figure.4-5-6, and Table.2, that shows the active and reactive power signals, Direct and quadratic signals with the traditional VC and the proposed VC-ILC in faulty conditions, we notice that:

- The Active power response time is minimized more than 84 % (1.65 s for classical VC instead 0.25 s for suggested VC-ILC). It is apparent that the new FTC (VC-ILC) controller improves the time response of the active power, (see figure 4a).
- The Active power overshoot is minimized more than 45 % (33 W for classical VC instead 18W for suggested VC-ILC) (see the zoom A of active power presented in figure 4b).

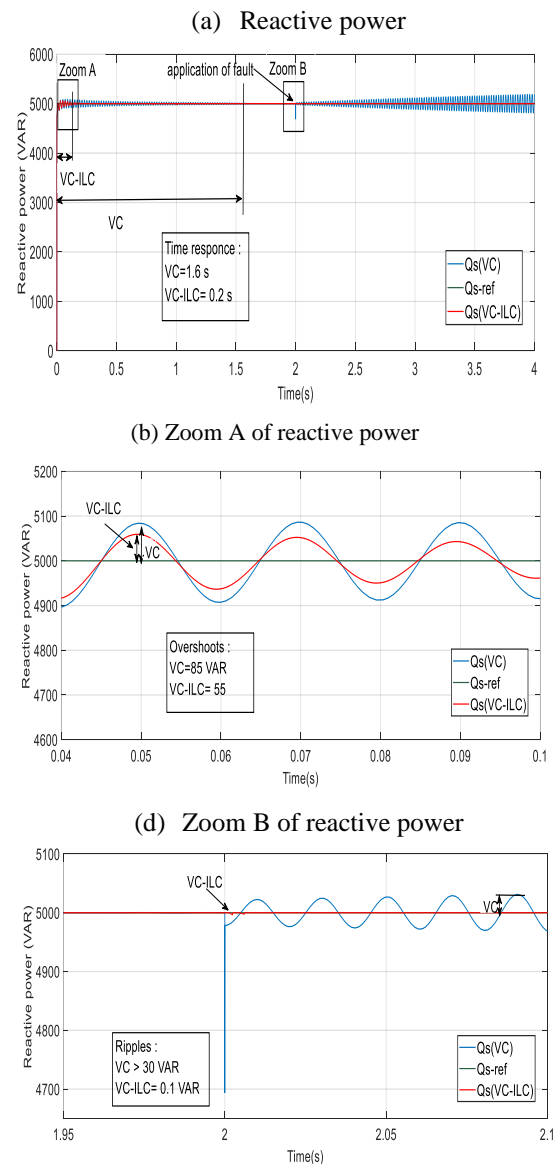


Fig. 5. Reactive power signals with VC and proposed VC-ILC controller in faulty conditions

- The response time (s) of the Reactive power is improved more than 87.5% (1.6 s for classical VC instead 0.2 s for suggested VC-ILC) as shown in figure 5a.
- The reactive power overshoot is minimized more than 35 % (85 VAR for classical VC instead 55 VAR for suggested VC-ILC) (see the zoom A of reactive power presented in figure 5b).
- The reactive power ripples is decreased for traditional VC from 30 VAR to 0.1 VAR when the suggested approach (VC-ILC) utilizing as described in the figure 5c). The suggested FTC has an improved dynamic, which minimizes the active and reactive power ripples and overshoots considerably. As a result of these characteristics, the new algorithm is appropriate for applications requiring specialized performance.

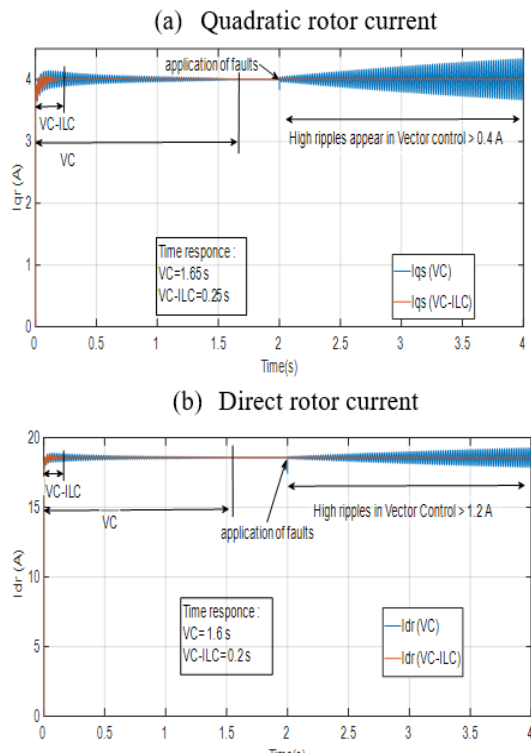


Fig. 6. Direct and Quadratic signals with VC and proposed VC-ILC controller in faulty conditions

- The ripples of the direct rotor current is minimized for traditional VC from 1.2 A to 0.1 A using suggested (VC-ILC) so enhancement for 91 % (see figure 6a).
- The response time of the direct rotor current is minimized more than 87.5 % (1.6 A for conventional VC instead 0.2 A for proposed VC-ILC) (see figure 6a).
- The response time (s) of the quadratic rotor current is improved more than 84% (1.65 s for conventional VC instead 0.25 s for proposed VC-ILC) as shown in the figure 6b).
- The ripples of the quadratic rotor current is reduced more than 87.5% (0.4 VAR for

conventional VC instead 0.05 VAR for proposed VC-ILC), (see figure 6b)

5.1. Robustness test

In order to evaluate the robustness of the suggested control approach, the values of inductances M , L_r and L_s are multiplied by 0.5, the value of the R_s and R_r are multiplied by 2. Figures.7 and 8 show the effects of parameters variation on the active and reactive power responses for the VC and VC-ILC controllers.

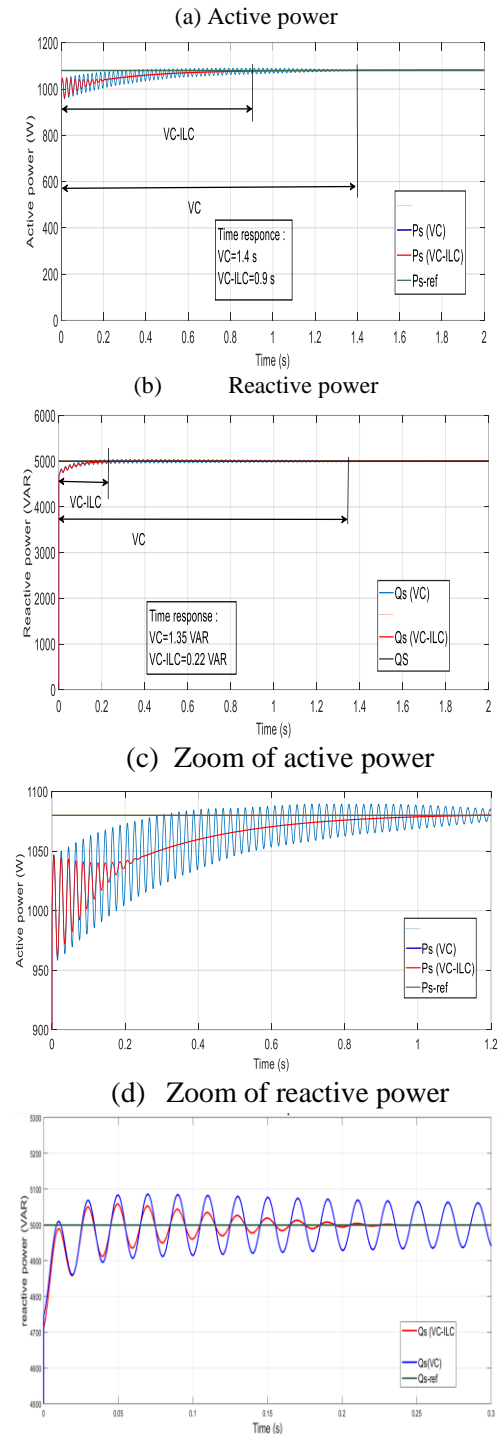


Fig. 7. Active and reactive power behaviour using VC and VC-ILC control with parameter variation.

Depending on Figure 7, we notice that these modifications have an evident influence on the active and reactive power curves, and the effect appears to be more noticeable for the VC control compared to the VC-ILC method. For example, the time response of the active power is improved from 1.4 s for traditional VC to 0.9 s using the suggested VC-ILC (see Figure 7 a). Thus, it can be concluded that the proposed VC-ILC is more robust than the conventional VC.

Table 3. Comparative results between VC and VC-ILC with parameter variation

Characteristics	VC	VC-ILC	improvement reduction ratio %
P_s Time response (s)	1.4	0.9	35
Q_s Time response (s)	1.35	0.22	83

Table 3 summarizes the major improvement of the suggested VC-ILC compared to the classical VC with parameter variation ($R_s \times 2$, $R_r \times 2$, $L_r \times 0.5$, $L_m \times 0.5$, $L_s \times 0.5$) we can get some notice:

- The Active power response time (s) is decreased for classical VC from 1.4s to 0.9s using suggested VC-ILC) so enhancement for 35 % as shown in figure 7a, 7c;
- The response time (s) of the Reactive power is reduced more than 83% (1.35s for conventional VC instead 0.22s using proposed VC-ILC) (see figure 7b, 7d).

6. CONCLUSION

A fault-tolerant control approach based on the combination between Vector Control (VC) and Iterative Learning Controller (ILC) for doubly fed induction generator to compensate the faults effect was described. The suggested technique is designed for making the DFIG tolerant to unanticipated faults. This technique seems to be an effective choice for improve power quality. The main contributions of this study are the decrease of ripple and overshoot, as well as the enhancement of response time, moreover, the ability of the proposed FTC (VC-ILC) to compensate the faults. Simulation results and table 2-3 present the major enhancement of the suggested FTC (VC-ILC) compared to the classical VC thus the proposed FTC (VC-ILC) is more efficient and has a higher likelihood of being utilized in electric drives compared to traditional VC controllers. In conclusion, the high effectiveness and robustness of the suggested approach can be useful for industrial implementation where the power quality is a

significant worry and the operating conditions are critical.

Author contributions: *research concept and design, O.B.D., A.D.; Collection and/or assembly of data, O.B.D.; Data analysis and interpretation, O.B.D.; Writing the article, O.B.D.; Critical revision of the article, M.H., S.Z., A.D.; Final approval of the article, S.Z., A.D.*

Declaration of competing interest: *The authors declare that they have no known competing financial interests or personal relationships that could have appeared to influence the work reported in this paper.*

REFERENCES

1. Farhoodne M, Azah M, Shareef H, Zayandehroodi H. Power quality impacts of high-penetration electric vehicle stations and renewable energy-based generators on power distribution systems. *Measurement* 2013; 46: 2423-2434. <https://doi.org/10.1016/j.measurement.2013.04.032>.
2. Abdelmalek S, Barazane L, Larabi A. An advanced robust fault-tolerant tracking control for a doubly fed induction generator with actuator faults. *Turkish Journal of Electrical Engineering and Computer Sciences* 2017; 25(2): 1346 – 1357. <https://doi.org/10.3906/elk-1508-16>.
3. Nazir MS, Wang Y, Mahdi AJ, Sun X, Zhang C, Abdalla AN. Improving the performance of doubly fed induction generator using fault tolerant control a hierarchical approach. *Applied Sciences* 2020; 10(3): 924. <https://doi.org/10.3390/app10030924>.
4. Lizarraga-Morales A, Rodriguez-Donate C, Cabal-Yepez E, Lopez-Ramirez M, Ledesma-Carrillo LM, Ferrucho-Alvarez ER. Novel FPGA-based methodology for early broken rotor bar detection and classification through homogeneity estimation. *IEEE Transactions on Instrumentation and Measurement* 2017; 66(7): 1760–1769. <https://doi.org/10.1109/TIM.2017.2664520>.
5. Mekki H, Benzineb O, Boukhetala D, Tadjine M, Benbouzid M. Sliding mode based fault detection, reconstruction and fault tolerant control scheme for motor systems. *ISA Transactions* 2015; 57: 340 – 351. <https://doi.org/10.1016/j.isatra.2015.02.004>.
6. Li-Ying H, Guang-Hong Y. Robust fault tolerant control based on sliding mode method for uncertain linear systems with quantization. *ISA Transactions* 2013; 52(5): 600–610. <https://doi.org/10.1016/j.isatra.2013.04.007>.
7. Nikoukhah R, Campbell SL, Drake K. An active approach for detection of incipient faults. *International Journal of Systems Science* 2010; 41(2): 241–257. <https://doi.org/10.1080/00207720903045817>.
8. Zhang Y, Jiang J. Bibliographical review on reconfigurable fault-tolerant control systems. *Annual Reviews in Control* 2008; 32(2): 229-252. <https://doi.org/10.1016/j.arcontrol.2008.03.008>.
9. Djeghali N, Ghanes M, Djennoune S, Barbot JP. Sensorless fault tolerant control for induction motors. *International Journal of Control, Automation and Systems* 2013; 11(3): 563–576. <https://doi.org/10.1007/s12555-012-9224-z>.
10. Lebreton C, Damour C, Benne M, Grondin-Perez B, Chabriet JP. Passive fault tolerant control of PEMFC air feeding system. *International Journal of Hydrogen*

Energy 2016; 41(34): 15615-15621.

<https://doi.org/10.1016/j.ijhydene.2016.06.210>

11. Corradini ML, Ippoliti G, Orlando G. Robust control of variable-speed wind turbines based on an aerodynamic torque observer. IEEE Transactions on Control Systems Technology 2013; 21(4): 1199–1206. <https://doi.org/10.1109/TCST.2013.2257777>.
12. Mesbahi T, Ghennam T, Berkouk EM. A doubly fed induction generator for wind stand-alone power applications (simulation and experimental validation). 2012 XXth International Conference on Electrical Machines 2012; 2028-2033. <https://doi.org/10.1109/ICEIMach.2012.6350161>.
13. Bouderbala M, Bossoufi B, Lagrioui A, Taoussi M, Aroussi HA, Ihedrane Y. Direct and indirect vector control of a doubly fed induction generator based in a wind energy conversion system. International Journal of Electrical and Computer Engineering 2018; 9(3): 1531-1540 <https://doi.org/10.11591/ijece.v9i3.pp1531-1540>.
14. Benbouhenni H, Boudjema Z, Belaïdi A. Direct vector control of a DFIG supplied by an intelligent SVM inverter for wind turbine system. Iranian Journal of Electrical and Electronic Engineering 2019; 15(1): <https://doi.org/10.22068/IJEEE.15.1.45>.
15. Qian W, Panda SK, Xu JX. Speed ripple minimization in PM synchronous motor using iterative learning control. IEEE Transactions on Energy Conversion 2005; 20: 53–61 <https://doi.org/10.1109/TEC.2004.841513>.
16. Houari A, Djeriou A, Saim A, Ait-Ahmed M, Machmoum M. Improved control strategy for power quality enhancement in standalone systems based on four-leg voltage source inverters. The Institution of Engineering and Technology 2017; 11(3): 515-523. <https://doi.org/10.1049/iet-pel.2017.0124>.
17. Becheri Houcine, Ismail K B, Bousmaha B, Abdelkader H, Tahar B. Vector control of wind turbine conversion chain variable speed based on DFIG using MPPT strategy. International Journal of Applied Engineering Research 2018; 13(7): 5404-5410.
18. Cherifi D, Miloud Y. Performance analysis of adaptive fuzzy sliding mode for nonlinear control of the doubly fed induction motor. Indonesian Journal of Electrical Engineering and Informatics 2018; 6(4): 436-447. <https://doi.org/10.11591/ijece.v6i1.605>.
19. Vas P. Parameter estimation, condition monitoring and diagnosis of electrical machines. Oxford Science Publications 1994.
20. Bonivento C, Isidori A, Marconi L, Paoli A. Implicit fault tolerant control: application to induction motors. Automatica 2004; 40(3): 355–371. <https://doi.org/10.1016/j.automatica.2003.10.003>.
21. Qian W, Panda SK, Xu JX. Torque ripple minimization in PM synchronous motors using iterative learning control. IEEE Transactions on Power Electronics 2004; 19(2): 272–279. <https://doi.org/10.1109/TPEL.2003.820537>.
22. Liu J, Li H, Deng Y. Torque ripple minimization of PMSM based on Robust ILC via adaptive sliding mode control. IEEE Transactions on Power Electronics 2018; 33(4): 3655-3671. <https://doi.org/10.1109/TPEL.2017.2711098>.



Oussama DJAIDJA

was born in M'sila, Algeria, in 1993. In 2016 he was received the Bs degree from University of M'sila, He received his Master Degree in Automatic from M'Sila University, Algeria, in 2018, He is currently a PhD student in M'sila University. His research interests include Fault tolerant control, control and power quality. He can

be contacted at email: oussama.djaidja@univ-msila.dz



Dr. Hemza MEKKI

was born in M'Sila, Algeria, on January 24, 1983. He received the engineering degree in electronic from the University of M'Sila, Algeria, in 2006. He received the degrees of Magister and doctorate on automatic from national polytechnic school, Algiers, Algeria, in 2009 and 2018 respectively. He is

currently a lecturer at the University of Mohamed Boudiaf of M'Sila. His research interests are fault tolerant control and diagnostic of electrical drive systems. He can be contacted at email: hemza.mekki@univ-msila.dz



Prof. Samir ZEGHLACHE

was born in Sétif, Algeria. He received his Engineer degree in Automatic from M'Sila University, Algeria, in 2006 and the Magister Diploma from Military Polytechnic School, - Bordj el Bahri- Algiers, Algeria, in 2009, all in Electrical Engineering. He received the doctorate degree in electronic

from the University of M'Sila, Algeria. In 2011, he joined M'Sila University, Algeria, where he works currently as lecturer. His research interests are non linear system control. He is the author and co-author of numerous articles on the faulttolerant control of vertical flight devices. In 2017, he created the first doctoral school in automatic in the history of the University of M'Sila. He can be contacted at email: samir.zeghlache@univ-msila.dz



Dr. Ali DJERIOUI

was born in M'sila, Algeria, in 1986. In 2009, he received the engineering degree in electrical engineering from the University of M'sila, Algeria. In 2011, he was graduated M.Sc. degree in electrical engineering from the Polytechnic Military Academy in Algiers, Algeria respectively where he is currently working

toward the Ph.D. degree in Electronic Instrumentation systems at the University of USTHB, Algiers, Algeria. His main interests are power converters, control and power quality. He can be contacted at email: ali.djeriou@univ-msila.dz